On-line FTIR as a novel tool to monitor Fenton process behavior

Noemí Merayo, Daphne Hermosilla*, Carlos Negro and Ángeles Blanco

Department of Chemical Engineering, Complutense University of Madrid, Facultad de Ciencias Químicas, Ciudad Universitaria s/n, 28040 Madrid, Spain.

* Corresponding author. Tel.: +34 91 394 4645; fax: +34 91 394 4243.

E-mail address: dhermosilla@quim.ucm.es (D. Hermosilla).

ABSTRACT

The efficiency of advanced oxidation processes is usually optimized by measuring the evolution of some water quality parameters sampling aliquots at pre-selected time intervals, such as particular undesired contaminants contents, or the reduction of chemical oxygen demand and total organic carbon. Besides providing good information regarding overall treatment performance and dynamics, this methodology also implies large analytical time consumption, and does not offer the actual full sequence of compounds appearing and disappearing during oxidation. On-line Fourier transform infrared spectroscopy is herein reported as a very useful tool for this purpose. In particular, it was successfully applied to monitoring the Fenton's oxidation of three model compounds (phenol, acetic acid, and oxalic acid) performed in continuous, providing precise control of the effect of reagents over time. Hydroxylation reactions resulted in the formation of hydroquinone and catechol as the main aromatic by-products being generated along the oxidation of phenol by the Fenton process. All phenolic substances (phenol, hydroquinone, benzoquinone, and catechol) were totally removed along the reaction. Carboxylic acids (oxalic and acetic mainly) were significantly present as final by-products of the oxidation process, highlighting their oxirecalcitrant behavior. On-line FTIR successfully enabled monitoring the Fenton process, and it provided a precise control of the effect of reagents along reaction time. Applications for a future on-line control of Fenton processes in industry may be developed in order to optimize the use of reagents and the potential combination with biological treatment stages; therefore reducing the operational cost of this advanced oxidation treatment.

Keywords: Advanced oxidation processes; Fenton method; Fourier transform infrared spectroscopy; treatment on-line monitoring; phenol.

1. Introduction

Advanced oxidation processes (AOPs) involving the *in situ* generation of highly reactive transitory species (e.g. H_2O_2, $OH^{\cdot}$, O_3, $O_2^{-\cdot}$) are taking advantage when conventional wastewater treatment techniques become insufficient to treat biorefractory contaminants [1-5]. Particularly, the method described by Fenton [6] is one of the most frequently used because it is generally more efficient, and implies a significant lower economical cost than other AOPs [2, 5, 7, 8].

The Fenton process is based on the electron transfer between hydrogen peroxide (H_2O_2) and ferrous ion (Fe^{2+}), which acts as a homogenous catalyst, generating hydroxyl radicals ($OH^{\cdot}$) that can degrade organic compounds [9]. These highly reactive radicals initiate the oxidative destruction of organic substances (RH) present in wastewater by hydroxyl radical addition or hydrogen atom abstraction reactions [5]. Organic free radicals ($R^{\cdot}$) are formed as transient intermediates that are further oxidized by hydroxyl radical, hydrogen peroxide, oxygen, ferric iron, and other oxidative intermediates; finally yielding stable oxidized products [5].

The optimization and process control of Fenton treatment and other AOPs has usually been undertaken by measuring certain water quality parameters (e.g. undesired contaminants contents, chemical oxygen demand, and/or total organic carbon removal) at certain time intervals. In addition, several techniques have widely been applied to characterize the sequence of organic compounds that are produced during the oxidative treatment using this discrete sampling protocol, such as high-performance liquid chromatography (HPLC) [10-12], gas chromatography-mass spectrometry (GC-MS) [13-14], Fourier transform infrared spectroscopy (FTIR) [15-16], or different combinations of them, or with other analytic techniques (e.g. ultraviolet-visible

spectrophotometry (UV-Vis), liquid chromatography–mass spectrometry (LC-MS), ion chromatography (IC), etc.) [17-21].

Particularly, FTIR has been previously applied to analyze the surface of catalysts and adsorbed substances along diverse AOPs treatments [22-25]. Gas samples have also been analyzed by FTIR to measure the generation of carbon dioxide (assimilable as mineralized carbon) in outlet gaseous streams of ozonation processes, which served as an indirect control parameter of the treatment [26]. In addition, FTIR has also been applied to control reactions in liquid samples identifying the compounds that are appearing and disappearing in the solution at preset time intervals [15-16]. All these methods enabling an indirect discrete control of the reaction involve great analytical time investment, and do not provide a full continuous characterization of the sequence of compounds that are produced in, or removed from the solution along the process. Furthermore, no reference for its on-line application has been reported to date.

On the other hand, membrane-introduction mass spectrometry (MIMS) has actually been applied to perform on-line measurements along photocatalytic processes [27]. Nevertheless, despite this methodology has been reported useful for monitoring these processes on-line, just volatile organic pollutants that are present in water can be effectively analyzed; whereas other highly polar substances could not be detected properly, such as some compounds that have been previously reported to be typically generated along the oxidation process of phenol [27].

Moreover, the current tendency of improving the combination of AOPs with biological technologies [28, 29] would surely welcome the application of advanced analytical methods to optimize the efficiency of every treatment step considering the predominant bio- or oxi- degradable nature of by-products. Therefore, the main objective of this essay was developing a suitable methodology of on-line monitoring the

evolution of the Fenton treatment of model organic compounds based on FTIR; which may ultimately allow the addition of reagents to be optimized, a further identification of the involved reactions, and the qualitative and quantitative determination of the by-products that are generated along the process.

2. Material and methods

2.1. Material and analytical methods

All used chemicals were of analytical grade and supplied by PANREAC S.A. (Barcelona, Spain) and Sigma-Aldrich (Highland, USA). Solutions were prepared in ultrapure water and kept in dark until use. 0.1 N H_2SO_4 and 0.1 N NaOH were used to adjust the pH value of the solution along the process.

The concentration of each tested organic compound (16 mmol of phenol, 14 mmol of oxalic acid, and 12 mmol of acetic acid in a total volume of 100 mL) was considered in order to achieve a good monitoring resolution of the process in the ReactIR iC10 device. Phenol was chosen as a model compound to perform this essay because its degradation behavior by several AOPs (Fenton process included) has widely been described previously [30-34], so it would perfectly serve to evaluate the proposed methodology. In addition, oxalic and acetic acids were also chosen due to its oxirecalcitrant nature [32].

All analyses were made according to the standard methods for the examination of water and wastewaters [35]. Chemical oxygen demand (COD) was measured by the colorimetric method at 600 nm using an Aquamate-spectrophotometer (Thermos Scientific AQA 091801, Waltham, USA); and hydrogen peroxide concentration was analyzed using the titanium-sulphate spectrophotometric method [36]. As residual hydrogen peroxide in the solution interferes with COD analysis, this interference was

corrected fitting the relationship between COD and hydrogen peroxide content to a second order polynomial equation ($DQO(H_2O_2) = -0.000020 \cdot [H_2O_2]^2 + 0.393239 \cdot [H_2O_2]$; $R^2 = 99.92\%$; $p = 0.0001$) [37].

Total organic carbon (TOC) was measured by the combustion-infrared method using a TOC/TN analyzer multi N/C® 3100 (Analytik Jena AG, Jena, Germany) with catalytic oxidation on cerium oxide at 850ºC. The integration of the information provided by the evolution of both COD and TOC along the oxidation treatment was assessed by calculating the mean oxidation number of organic carbon ($MOC = 4 \cdot [1-(COD/TOC)]$, considering both COD and TOC in molar units)[32].

Phenol and reaction intermediates were complementary measured by High Pressure Liquid Chromatography (Model L920, Varian, CA, USA) with diode array (PDA) detection. Acetonitrile - water (15%:85%), and (50%:50%) were used as the eluent for aromatics and carboxylic acids, respectively. Sample injections of 20 µL were separated on a C-18 column (Vidac 250 mm x 4.6 mm ID x 5µm) at 30ºC. The target compounds were measured at the following wavelengths: hydroquinone (290 nm), benzoquinone (245 nm), catechol (280 nm), phenol (270 nm), acetic acid and oxalic acid (200 nm).

2.2. FTIR analytical device

ReactIR iC10 (Mettler-Toledo, Columbia, USA) is a real-time *in situ* reaction monitoring system, based on FTIR spectrometry, that is able to provide all the organic chemical species that are present in the solution as the reaction is being performed. The FTIR spectrometer uses a mercury-cadmium telluride (MCT) detector that is cooled by liquid nitrogen; and measurements are optically taken using a diamond-tipped probe with a 1 meter long fibre-optic conduit. This system was purged using instrumental-

grade air; therefore preventing water vapour from collecting inside the optics, which may obscure spectral data otherwise.

Data acquisition was performed from 2000 to 650 cm^{-1} with an 8 cm^{-1} nominal resolution. 256 scans were co-added for each spectrum. A background of pure water was carried out using the same resolution and scanning conditions of the trials before each spectral record. These water spectra were subtracted from each corresponding resulting on-line spectra.

Real-time component analyses were performed using ConcIRT software (Mettler-Toledo, Columbia, USA), which applies the curve-resolution mathematical algorithm for grouping wavenumber values that change absorbance intensity in the same way. This software calculates the associated component spectrum and the relative concentration profile in terms of absorbance units for each group; and it re-analyzes and updates all spectra and concentration profiles as each new reaction spectrum is acquired. In short, calculation results evolve as the reaction proceeds, and every organic component (reagent, intermediate or product) that is present in the solution is detected in real-time; and its relative concentration profile is therefore provided.

2.3. Experimental procedure

Experiments were performed in the dark inside a 500mL glass reactor where 100mL of the solution were continuously stirred (300rpm) with a magnetic device at room temperature (≈20-25 ºC). All experiments were repeated three times. pH = 2.8 (± 0.2) was kept constant along the process. pH adjustment was required until this 2.8 value was monitored stable and no further regulation was necessary. The concentrations of reagents were chosen to meet the following ratios: $[H_2O_2]$ / COD_0 = 2.15, and $[H_2O_2]$

/ [Fe^{2+}] = 37.5; as these reaction conditions have previously been reported to produce optimal Fenton treatment results for the target substances [30, 32].

The required amount of ferrous sulphate was added in batch mode after the initial pH value was adjusted. Hydrogen peroxide was thereafter added in continuous mode, so all the designed dosage of this reagent was supplied after 120 minutes of reaction. In fact, the continuous addition of H_2O_2 has already been reported to provide better results than batch mode in previous trials of this process [31, 37]. In addition, it also allows a better understanding of the process enabling the use of the added quantity of H_2O_2 (milimol), rather than reaction time, as an indicator of the progress and evolution of oxidation.

Additional trials were performed in equal conditions in which aliquots of the solution were withdrawn with a syringe in order to monitor the overall progress of the reaction in terms of COD removal and H_2O_2 consumption. This way, volume changes did not alter FTIR-monitoring runs. These samples were neutralized to pH = 9.0 with 40% NaOH, mixed, and centrifuged for 15 min at 2000 rpm, before collecting the supernatant where COD and [H_2O_2] were determined.

The ReactIR iC10 probe placed inside the reactor monitored the whole reaction progress in real time. In order to properly read and calibrate spectral results, the characteristic bands of the main compounds that were expected to be produced during the Fenton treatment of the target substances were crosschecked using the available information found in bibliography (Table A.1), and our own collected spectra from conveniently prepared control solutions containing just one of these compounds (Figures A.1 and A.2), which have been included in Appendix A. Despite the similarity of some by-products of the reaction, the full interpretation of the generated complex

spectra recorded during the trials was successfully achieved thanks to the mathematical algorithms provided by ConcIRT software.

3. Results and discussion

3.1. Degradation of phenol by the Fenton process

All three repetitions of every performed experiment reproduced the same results, and there were not found meaningful differences among them.

Spectra within the region of 650 to 2000 cm^{-1} continuously increased during H_2O_2 addition until 60 mmol of H_2O_2 were added in total, when the highest overall absorbance was reached. Subsequently thereafter, the overall spectra began to decrease and all peaks progressively became smoother (Figure 1).

After the first addition of H_2O_2, the color of the solution instantaneously changed from colorless to dark brown (almost black) due to the oxidation of ferrous to ferric ion, and the generation of quinones (i.e. hydroquinone and benzoquinone, Figure 2) in redox equilibrium [31, 33], which are more toxic than phenol itself [31]. This dark color gradually lost its intensity thereafter, and a pale orange color remained after adding a total 160 mmol of H_2O_2 (when its ratio to the initial amount of phenol was 10) because quinones have already been degraded; as well as due to the remaining presence of several by-products of acid formation stages (oxalic acid, mainly) [32-33] that are able to reduce ferric back to ferrous iron [38]. Similar color changes have been addressed before [33, 39]. Furthermore, HPLC analyses confirmed these FTIR results.

The evolution of MOC along treatment (Figure 2) also supports this affirmation linearly changing from an initial value of -0.67, which is characteristic for phenol, to ≈3, which has previously been addressed to a mix of carboxylic acids where oxalic (MOC = 3) predominates [32]; and then it remained constant thereafter.

The concentration profile of phenolic compounds resulted mainly integrated by phenol itself and some products that are generated by its hydroxylation, namely hydroquinone, benzoquinone [31, 33, 40] and catechol (Figure 2). On the other hand, resorcinol was not actually found along the Fenton oxidation of phenol. In fact, its formation would rather be implausible based upon the substitution rules of organic chemistry [33]; and it may anyhow occur in an about one thousand times lower frequency than the generation of catechol and hydroquinone [34].

The absorbance concentration profile of phenolic compounds logically increased as phenol was added to the solution; and it also grew again after the addition of H_2O_2 because other phenolic intermediate compounds of the reaction were newly formed (Figure 2). During the reaction, this phenolic mix totally disappeared when the concentration ratio between the added H_2O_2 and the initially supplied amount of phenol was close to 8, coinciding with previously reported results on the Fenton oxidation of phenol and nitrophenol, when a MOC value characteristic of the predominant presence of carboxylic acids (≈2.5-3) was kept more or less constant as the reaction progresses (Figure 2) [32].

Achieving the total degradation of hydroquinone is of environmental concern due to its high toxicity, which is several orders of magnitude higher than the attributed to phenol itself [29]. On the other hand, catechol also resulted totally removed at the end of the reaction, as it has been clearly addressed by HPLC measurements. Nevertheless, catechol is highly biodegradable [41, 42]; thus, it might be further treated by biological technologies, which are, in general, cheaper treatments than AOPs.

Furthermore, previous results reporting a significant much higher production of catechol than hydroquinone along the process were confirmed [33-34], as it results from comparing the concentration profiles of both compounds in Figure 2. In fact, the

production of catechol resulted a 100% higher than the measured for quinones by HPLC. In short, catechol and hydroquinone were initially formed as phenol disappeared; and then, they began to be gradually degraded competing with their own further formation as phenol was still being oxidized.

In addition, phenol decreased its concentration in the solution faster than the other newly generated phenolic intermediates (hydroquinone, benzoquinone, and catechol) of the reaction (comparing Figures 2 and 3); which is also in accordance to previous scientific reports [32-34]. Only a 4% of phenol remained after adding a ratio of H_2O_2 to phenol of 3.9; results that were further confirmed by HPLC analyses.

At this point, the removal of COD was higher than 50%, and it did not show further lineal progress (Figure 3). Finally, phenol resulted totally degraded when the aggregated concentration of H_2O_2 reached 5.6 times the initial amount of added phenol, and the reduction of the COD was close to a 75%; showing a further asymptotic evolution because of the growing presence of carboxylic acids, which are more difficult to oxidize. Hereafter, the mix of phenolic compounds remaining in the solution was mainly made up by hydroquinone and catechol (Figure 2), which absorbance concentration profile quickly decreased until the ratio between the total added H_2O_2 and the initial amount of phenol was close to 6.5. Then, its abatement thereafter progressed smooth, and its total degradation was finally achieved when this ratio arrived to about 8, as confirmed by HPLC determinations.

Some carboxylic acids remained in the solution at the end of the process as the main persistent by-products of the oxidation treatment of phenol (Figure 1); although they are also considered highly biodegradable and might be further treated by biological processes [41, 42]. Oxalic, acetic, and formic acids were identified as the resultant products of an acid formation stage within the process. Its presence and persistence was

also confirmed by HPLC measurement, and MOC and COD behavior assessment (Figures 2 and 3), as just stated before. That is, its presence resulted constant after the ratio of total added H_2O_2 to the initial amount of phenol reached a value close to 8, which was accurately measured by HPLC; and also confirmed by a non further change of MOC from characteristic values previously addressed for carboxylic acids mix [32], although COD was still slightly being removed (Figures 2 and 3).

In short, carboxylic acids were probably formed by ring-opening reactions that take place within degradation stages of some aromatic intermediate products of the reaction [32-33]. Whilst the presence of oxalic acid was detected from almost the beginning of the reaction (Figure 2), when the ratio of total added [H_2O_2] to the initial concentration of phenol was just 1.8; acetic and formic acids presence was noticed in the solution when this ratio reached 6.25, suggesting that these two carboxylic acids may be generated by the degradation of some other intermediate reaction by-products.

All these carboxylic acids that are inevitably formed during the oxidative degradation of phenol are more or less recalcitrant to its further Fenton advanced oxidation treatment [1, 16]; so they will hereafter be considered as oxirecalcitrant compounds [32]. In fact, this limited capacity to degrade carboxylic acids is one of the main drawbacks for achieving the total mineralization of phenol by Fenton's reagent [32, 33]. Therefore, the main objective of AOPs based treatment steps might be defined as controlling the process until a maximum biodegradability threshold is achieved in order to combine this treatment with a cheaper posterior biological stage [43].

In summary, a final 94% reduction of the COD was achieved (Figure 3), which is even higher than previously reported results [30, 32]. The continuous addition of H_2O_2, which has previously been proved to enhance the removal of COD in comparison to batch mode [37], as well as the steady thorough control of the reaction conditions that

was performed, have surely served well to achieve this very successful result. The 6% remaining COD was held by the remaining mix of oxirecalcitrant by-products, oxalic and other carboxylic acids, mainly.

3.2. Fenton treatment of acetic acid

When trying to oxidize acetic acid by Fenton's reagent, the initial addition of $FeSO_4 \cdot 7H_2O$ resulted in a colorless solution because the high production of a complex that is formed between acetic acid and ferrous iron drastically reduced the presence of both compounds in the solution (Figure 4). As H_2O_2 was thereafter added, the concentration of this complex began to decrease, and the solution turned to an orange-reddish color as ferric ion was generated [38], which further induced the formation of an acetic acid-ferric iron complex. The formation of this complex is stronger than the acetic acid-ferrous iron one [32], but it was not detected by FTIR in the spectral region under study (Figure 5). Nevertheless, the clearly noticed orange color of the solution, and the very limited figures of COD reduction, clearly suggest the presence of this ferric-acetic acid complex, as it has previously been reported [32].

The reaction may be considered finished when the ratio between the added concentration of H_2O_2 and the initial amount of supplied acetic acid reached 4.8. At this moment, the organic-ferrous iron complex disappeared because there was not any available Fe^{2+} to form more $OH\cdot$ that might have further continued the oxidation process, and the acetic acid-ferric iron complex (not visible to FTIR) and formic acid (Figure 5) remained in the solution as the final result of the attempted degradation of acetic acid by the Fenton's reagent [44-45]. Final COD reduction figures were just about a 9% due to the above mentioned oxirecalcitrant nature of this type of chemicals. In fact, these poor treatment results fully agree with other previously reported ones [32].

3.3. Fenton oxidation of oxalic acid

A constant weak green-yellow color predominated in the solution along the treatment of oxalic acid by Fenton's reagent; even after H_2O_2 was added. Therefore, ferrous to ferric ion oxidation was occurring at a very low pace; being oxalic acid itself contributing to reduce ferric back to ferrous [38]. This process partially slowed the oxidative process down because some H_2O_2 was being wasted on oxidizing ferrous iron back to ferric one.

In short, Fenton oxidation did not produce any degradation of oxalic acid (Figure 6). In fact, great Fe^{2+} losses have previously been attributed to the formation of a strong oxalic-ferrous complex, which consequently hinders the oxidation process to progress [32]. Although this oxalic-ferrous complex was not detected by the FTIR probe, probably due to its very close likeness to other oxalic compounds, the oxidation process resulted similarly hindered.

In fact, the absorbance concentration profile of oxalic acid did not show any change after increasing the addition of H_2O_2 (Figure 6); although it significantly decreased previously, just after adjusting the pH (adding 40% NaOH), because oxalic acid and oxalate anion contents depend on the pH value of the solution [46]. That is, oxalate anion was formed as pH increased, as it is detailed in Figure 7. Whereas the characteristic wavenumber peaks of oxalic acid (1733 and 1232 cm^{-1}) gradually decreased during the addition of 40% NaOH until its content stabilized at a very constant final value [46]; those typical peaks of oxalic anion (1571 and 1310 cm^{-1}) showed up, and correspondingly increased its absorbance record, after NaOH was added, until its content reached a steady state as well [46].

Summing up, the total removal of the COD that was achieved in the treatment of oxalic acid by Fenton's reagent resulted lower than the 7%. This result totally meets previously reported results [31-32], which also suggested that it is the variation of pH, rather than the oxidative treatment itself, which is the responsible of this reduction of the COD. In fact, this slight percentage of COD removal was surely the result of the final precipitation of oxalic acid when pH was turned to 9 adding NaOH at the end of the reaction aiming to remove iron precipitating its hydroxides.

4. Conclusions

The above reported results clearly show that the effectiveness of an oxidation process may successfully be assessed by FTIR, implying a significant reduction of the time devoted for analyses in comparison to other methodologies. In addition, it has been shown that the results obtained by FTIR were in total agreement with those previously reported using chromatographic analyses. That is, aliphatic organic compounds were not easily degraded with this type of treatment, whereas phenol resulted totally removed.

The quality and quantity of reaction intermediates that were produced during the oxidative degradation of phenol were fully assessed, and the mechanisms that were involved were also well observed. Thanks to receiving real-time information, this procedure allowed a precise control of the effects of reagents on the treated substances, which furthermore enabled optimizing the quantities of reagents required in the process. This may further enable the successful optimization of the treatment combination of AOPs with biological technologies, as the reaction moment where oxirecalcitrant (but biodegradable) substances were mainly present in the solution was clearly identified.

Acknowledgements

This research was developed in the frame of the projects "AQUAFIT4USE" (211534), funded by the European Union; "AGUA Y ENERGÍA" (CTM2008-06886-C02-01), and "OXIPAPEL" (CIT-310000-2008-15), both funded by the Ministry of Science and Innovation of Spain. N. Merayo's participation was sponsored by a Ph.D. grant from the Ministry of Economy and Competitivity of Spain.

Appendix A. Spectral characteristics of the chemical species produced along the Fenton oxidation treatment of phenol

References

[1] R.J. Bigda, Consider Fenton's chemistry for wastewater treatment, Chem. Eng. Prog. 91 (1995) 62-66.

[2] S. Esplugas, J. Giménez, S. Contreras, E. Pascual, M. Rodríguez, Comparison of different advanced oxidation processes for phenol degradation, Water Res. 36 (2002) 1034-1042.

[3] C. Comninellis, A. Kapalka, S. Malato, S.A. Parsons, I. Poulios, D. Mantzavinos, Advanced oxidation processes for water treatment: advances and trends for R&D, J. Chem. Technol. Biotechnol. 83 (2008) 769-776.

[4] W.H. Glaze, J.W. Kang, D.H. Chapin, The Chemistry of Water-Treatment Processes Involving Ozone, Hydrogen-Peroxide and Ultraviolet-Radiation, Ozone-Sci. Eng. 9 (1987) 335-352.

[5] C.P. Huang, C. Dong, Z. Tang, Advanced chemical oxidation: its present role and potential future in hazardous waste treatment, Waste Manag. 13 (1993) 361-377.

[6] H.J.H. Fenton, Oxidation of tartaric acid in presence of iron, J. Chem. Soc. 65

(1894) 899-910.

[7] F.J. Rivas, F.J. Beltrán, F. Carvalho, B. Acedo, O. Gimeno, Stabilized leachates: sequential coagulation-flocculation plus chemical oxidation process, J. Hazard. Mater. 116 (2004) 95-102.

[8] W.Z. Tang, Physicochemical treatment of hazardous wastes, Lewis Publishers, Boca Raton, FL, 2004.

[9] F. Harber, J.J. Weiss, The catalytic decomposition of Hydrogen Peroxide by iron salts, J. Amer. Chem. Soc. 45 (1934) 338-351.

[10] J. Dzengel, J. Theurich, D.W. Bahnemann, Formation of Nitroaromatic Compounds in Advanced Oxidation Processes: Photolysis versus Photocatalysis Environ. Sci. Technol. 33 (1999) 294-300.

[11] K. Vinodgopal, Hydroxyl radical-mediated advanced oxidation processes for textile dyes: a comparison of the radiolytic and sonolytic degradation of the monoazo dye Acid Orange 7, J. Peller, Res. Chem. Intermed. 29, 3 (2003) 307–316.

[12] H. Wang, J. Wang, Electrochemical degradation of 2,4-dichlorophenol on a palladium modified gas-diffusion electrode, Electrochim. Acta 53 (2008) 6402–6409.

[13] J. Poerschmann, U. Trommler, Pathways of advanced oxidation of phenol by Fenton's reagent—Identification of oxidative coupling intermediates by extractive acetylation, J. Chromatogr. A 1216 (2009) 5570–5579.

[14] C. Justino, A.G. Marques, K.R. Duarte, A.C. Duarte, R. Pereira, T. Rocha-Santos, A.C. Freitas, Degradation of phenols in olive oil mill wastewater by biological, enzymatic, and photo-Fenton oxidation, Environ Sci Pollut Res 17 (2010) 650–656.

[15] J. Araña, E. Tello Rendón, J.M. Doña Rodríguez, J.A. Herrera Medián, O. González Díaz, J. Pérez Peña, Highly concentrated phenolic wastewater treatment by the Photo-Fenton reaction, mechanism study by FTIR-ATR, Chemosphere 44 (2001)

1017-1023.

[16] O. Abbas, C. Rebufa, N. Dupuy, J. Kister, FTIR—Multivariate curve resolution monitoring of photo-Fenton degradation of phenolic aqueous solutions. Comparison with HPLC as a reference method, Talanta 77 (2008) 200–209.

[17] I. Udrea, C. Bradu, Ozonation of Substituted Phenols in Aqueous Solutions over $CuO\text{-}Al_2O_3$ Catalyst. Ozone-Sci. Eng. 25 (2003) 335-343.

[18] L. Carlos, D. Fabbri, A.L. Capparelli, A. Bianco Prevot, E. Pramauro, F.S. García Einschlag, Intermediate distributions and primary yields of phenolic products in nitrobenzene degradation by Fenton's reagent, Chemosphere 72 (2008) 952–958.

[19] L. Carlos, D. Fabbri, A.L. Capparelli, A. Bianco Prevot, E. Pramauro, F.S. García Einschlag, Effect of simulated solar light on the autocatalytic degradation of nitrobenzene using Fe^{3+} and hydrogen peroxide, J. Photochem. Photobiol. A: Chem. 201 (2009) 32–38.

[20] L.G. Devi, K.S.A. Raju, S.G. Kumar, Photodegradation of methyl red by advanced and homogeneous photo-Fenton's processes: A comparative study and kinetic approach, J. Environ. Monit. 11, 7 (2009) 1397-1404.

[21] B. Kayan, B. Gözmen, M. Demirel, A.M. Gizir, Degradation of acid red 97 dye in aqueous medium using wet oxidation and electro-Fenton techniques, J. Hazard. Mater. 177 (2010) 95–102.

[22] L. Palmisano, M. Schiavello, A. Sclafani, G. Martra, E. Borello, S. Coluccia, Photocatalysic oxidation of phenol on TiO_2 powders. A Fourier transform infrared study, Appl. Catal. B 3 (1994) 117-132.

[23] M.B. Sayed, ^{1}H-NMR, UV-Visible, and FT-IR Spectral Analyses for the Conflicting Impacts of Proton Mobility and H-Bonding Association on the Mesomeric Structure in Azopyrogallol, Catechol, Resorcinol, Quinol, and Phenol Derivatives of

Melamine, Ind. Eng. Chem. Res. 43 (2004) 4822-4826.

[24] P.Z. Araujo, C.B. Mendive, L.A. García Rodenas, P.J. Morando, A.E. Regazzoni, M.A. Blesa, D. Bahnemann, FT-IR–ATR as a tool to probe photocatalytic interfaces, Colloids Surf. A Physicochem. Eng. Asp. 265 (2005) 73–80.

[25] S. Horikoshi, T. Miura, M. Kajitani, H. Hidaka, N. Serpone, A FT-IR (DRIFT) study of the influence of halogen substituents on the TiO_2-assisted photooxidation of phenol and *p*-halophenols under weak room light irradiance, J. Photochem. Photobiol. A: Chem. 194 (2008) 189–199.

[26] S.A. Carr, R.B. Baird, Mineralization as a mechanism for TOC removal: study of ozone/ozone-peroxide oxidation using FT-IR Water Res. 34, 16 (2000) 4036-4048.

[27] R.F.P. Nogueira, R.M. Alberici, M.A. Mendes, W.F. Jardim, M.N. Eberlin, Photocatalytic Degradation of Phenol and Trichloroethylene: On-Line and Real-Time Monitoring via Membrane Introduction Mass Spectrometry, Ind. Eng. Chem. Res. 38 (1999) 1754-1758.

[28] D. Mantzavinos, E. Psillakis, Enhancement of biodegradability of industrial wastewaters by chemical oxidation pre-treatment, J. Chem. Technol. Biotechnol. 79 (2004) 431-454.

[29] I Oller, S. Malato, J.A. Sánchez-Pérez, W. Gernjak, M.I. Maldonado, L.A. Pérez-Estrada, C. Pulgarín, Reduction in residual COD in biologically treated paper mill effluents by means of combined ozone and ozone/UV reactor stages, Catal. Today 122 (2007) 150–159.

[30] V. Kavitha, K. Palanivelu, The role of ferrous ion in Fenton and photo-Fenton processes for the degradation of phenol, Chemosphere 55 (2004) 1235-1243.

[31] J.A. Zazo, J.A. Casas, A.F. Mohedano, M.A. Gilarranz, J.J. Rodríguez, Chemical Pathway and Kinetics of Phenol Oxidation by Fenton's Reagent, Environ. Sci. Technol.

39 (2005) 9295-9302.
[32] D. Hermosilla, M. Cortijo, C.P. Huang, The role of iron on the degradation and mineralization of organic compounds using conventional Fenton and photo-Fenton processes, Chem. Eng. J. 155 (2009) 637–646.
[33] M.S. Yalfani, S. Contreras, F. Medina, J. Sueiras, Phenol degradation by Fenton's process using catalytic in situ generated hydrogen peroxide, Appl. Catal. B 89 (2009) 519–526.
[34] R.F.F. Pontes, J.E.F. Moraes, A. Machulek Jr., J.M. Pinto, A mechanistic kinetic model for phenol degradation by the Fenton process, J. Hazard. Mater. 176 (2010) 402–413.
[35] APHA, AWWA, WPCF (Eds.), Standard methods for the examination of water and wastewater, Washington DC, 1989.
[36] H. Pobiner, Determination of hydroperoxides in hydrocarbon by conversion to hydrogen peroxide and measurement by titanium complexing, Anal. Chem. 33 (1961) 1423-1428.
[37] D. Hermosilla, M. Cortijo, C.P. Huang, Optimizing the treatment of landfill leachate by conventional Fenton and photo-Fenton processes, Sci. Total Environ. 407 (2009) 3473-3481.
[38] S.E. Manahan, Environmental Chemistry, CRC Press, Boca Ratón, 2010.
[39]V. Kavitha, K. Palanivelu, Degradation of 2-Chlorophenol by Fenton and Photo-Fenton Processes—A Comparative Study, J. Environ. Sci. Heal. A 38 (2003) 1215-1231.
[40] H. Kusic, N. Koprivanac, A.L. Bozic, Photo-assisted Fenton type processes for the degradation of phenol: A kinetic study, Chem. Eng. J. 123 (2006) 127-137.
[41] M. D. Zeyaullah, A. S. Abdelkafe, W. B. Zabya, A. Ali, Biodegradation of

1 catechols by micro-organisms – A short review, Afr. J. Biotechnol. 8 (2009) 2916-2922.
2 [42] L. Pramparo, M. E. Suárez-Ojeda, J. Pérez, J. Carrera, Kinetics of aerobic
3 biodegradation of dihydroxybenzenes by a p-nitrophenol-degrading activated sludge,
4 Bioresour. Technol. 110 (2012) 57–62.
5 [43] D. Hermosilla, N. Merayo, R. Ordóñez, A. Blanco, Optimization of conventional
6 Fenton and ultraviolet-assisted oxidation processes for the treatment of reverse osmosis
7 retentate from a paper mill, Waste Manage. 32 (2012) 1236–1243.
8 [44] S. Kim, A. Vogelpohl, Degradation of Organic Pollutants by the Photo-Fenton-
9 Process, Chem. Eng. Technol. 21 (1998) 187-191.
10 [45] M.I. Stefan, J.R. Bolton, Mechanism of the Degradation of 1,4-Dioxane in Dilute
11 Aqueous Solution Using the UV/Hydrogen Peroxide Process, Environ. Sci. Technol. 32
12 (1998) 1588-1595.
13 [46] I.R. Moraes, F.C. Nart, Sulfate ions adsorbed on Au(hkl) electrodes: in situ
14 vibrational spectroscopy, J. Electroanal. Chem. 461 (1999) 110–120.
15 [47] Y.M. Jung, Characterization of pH-Dependent IR Spectra of Oxalic Acid:
16 Comparison of Self-Modeling Curve Resolution Analysis with Calculation of IR
17 Frequencies, Bull. Korean Chem. Soc. 24, 9 (2003) 1410-1412.
18 [48] B. Jin, P. Liu, Y. Wang, Z. Zhang, Y. Tian, J. Yang, S. Zhang, F. Cheng, Rapid-
19 Scan Time-Resolved FT-IR Spectroelectrochemistry Studies on the Electrochemical
20 Redox Process, J. Phys. Chem. B 111 (2007) 1517-1522.
21 [49] J. Araña, J.M. Doña Rodríguez, O. González Díaz, J.A. Herrera Melián, C.
22 Fernández Rodríguez, J. Pérez Peña, The effect of acetic acid on the photocatalytic
23 degradation of catechol and resorcinol, Appl. Catal. A Gen. 299 (2006) 274–284.
24 [50] H. Gulley-Stahl, P.A. Hogan II, W.L. Schmidt, S.J. Wall, A. Buhrlage, A.A.
25 Bullen, Surface Complexation of Catechol to Metal Oxides: An ATR-FTIR,

Adsorption, and Dissolution Study, Environ. Sci. Technol. 44 (2010) 4116–4121.

[51] F.C. Nart, T. Iwasita, M. Weber, Sulfate adsorption on well-define Pt(100) electrodes, Electrochim. Acta 39, 13 (1994) 2093-2096.

[52] R.T.S. Muthu Lakshmi, M.K. Vyas, A.S. Brar, I.K. Varma, Synthesis and characterization of sulphonated PEES copolymers by NMR spectroscopy, Eur. Polym. J. 42 (2006) 1423–1432.

[53] M.M. Hasani-Sadrabadi, S.H. Emami, H. Moaddel, Preparation and characterization of nanocomposite membranes made of poly(2,6-dimethyl-1,4-phenylene oxide) and montmorillonite for direct methanol fuel cells, J. Power Sources 183 (2008) 551–556.

Table A.1. Characteristic wavenumber peaks of relevant organic compounds that are produced during the Fenton oxidation of phenol, oxalic acid and acetic acid.

Wavenumber (cm^{-1})									
Phenol	Hydroquinone	Resorcinol	Catechol	Benzoquinone	**Oxalic acid**	**Acetic acid**	Formic acid	$FeSO_4 \cdot 7H_2O$	**References**
					1738				[47]
						1707			[16]
				1638					[48]
					1621				[47]
1595		1604	1604	1599					[16,22,25,49-51]
					1574 (anion)				[47]
1501									[16, 22, 25]
1475	1472								[16, 22, 25]
						1410			[16]
		1381							[49]
			1379						[49-50]
1372									[16, 22, 25]
	1367								[16]
					1310 (anion)				[47]
						1292			[16]
1235					1232				[16, 22, 25, 47]
					1226				[35]
			1200						[16, 49, 50]
								1089	[51-53]
809									[16, 22, 25]
752									[16, 22, 25]

Figure captions

Figure A.1. FTIR spectra of main inorganic and aliphatic compounds that are used and may be produced in the oxidation of phenol by the Fenton process.

Figure A.2. FTIR spectra of main aromatic chemicals that may be produced in the oxidation of phenol by the Fenton process.

Figure 1. Evolution of FTIR-spectra along a continuous hydrogen peroxide addition in the Fenton oxidation of phenol. The presence evolution of carboxylic acids is highlighted, and a turned around graph is also shown in small detail. (Reaction conditions: room temperature (≈ 20-25 ºC); pH = 2.8 ± 0.2; 16 mmol phenol; $[H_2O_2]$ / COD_0 = 2.15; $[H_2O_2]$ / $[Fe^{2+}]$ = 37.5).

Figure 2. Absorbance profiles for main by-products, and evolution of the MOC along a continuous hydrogen peroxide addition in the Fenton oxidation of phenol (Reaction conditions: room temperature (≈ 20-25 ºC); pH = 2.8 ± 0.2; 16 mmol phenol; $[H_2O_2]$ / COD_0 = 2.15; $[H_2O_2]$ / $[Fe^{2+}]$ = 37.5).

Figure 3. Smooth absorbance concentration profiles of phenol, and evolution of the removal of the COD along the Fenton oxidation of phenol considering all its three typical detection wavenumbers (752, 809, and 1501 cm^{-1}). Note: 1= addition of reagents; 2= progressive removal of phenol; 3= after the total removal of phenol.

Figure 4. Concentration profiles of acetic acid, formic acid and organic-iron complexes during the degradation of acetic acid by Fenton´s reagent. (Reaction conditions: 12 mmol acetic acid, pH = 2.8 ± 0.2, $[H_2O_2]/[Fe^{2+}]$ = 37.5).

Figure 5. FTIR spectra resulting for deionised water, phenol, acetic acid, and oxalic acid with and without the presence of ferric chloride trihydrate.

Figure 6. Evolution of FTIR spectra in the span ranging from 2000 to 800 cm^{-1} (A), and concentration profiles of oxalic acid and oxalate (B) along the Fenton oxidation of oxalic acid. (Reaction conditions: 14 mmol oxalic acid, pH = 2.8 ± 0.2, $[H_2O_2]/[Fe^{2+}]$ = 37.5).

Figure 7. Absorbance concentration profiles for characteristic wavenumber values of oxalic acid (1733 and 1232 cm^{-1}) and its anion (1571 and 1310 cm^{-1}) considering the following pH turns: (A) natural pH of an oxalic acid solution, (B) 40% NaOH addition to increase pH, and (C) pH values at which oxalic forms are stabilized (> 9.0).

FIGURE A.1

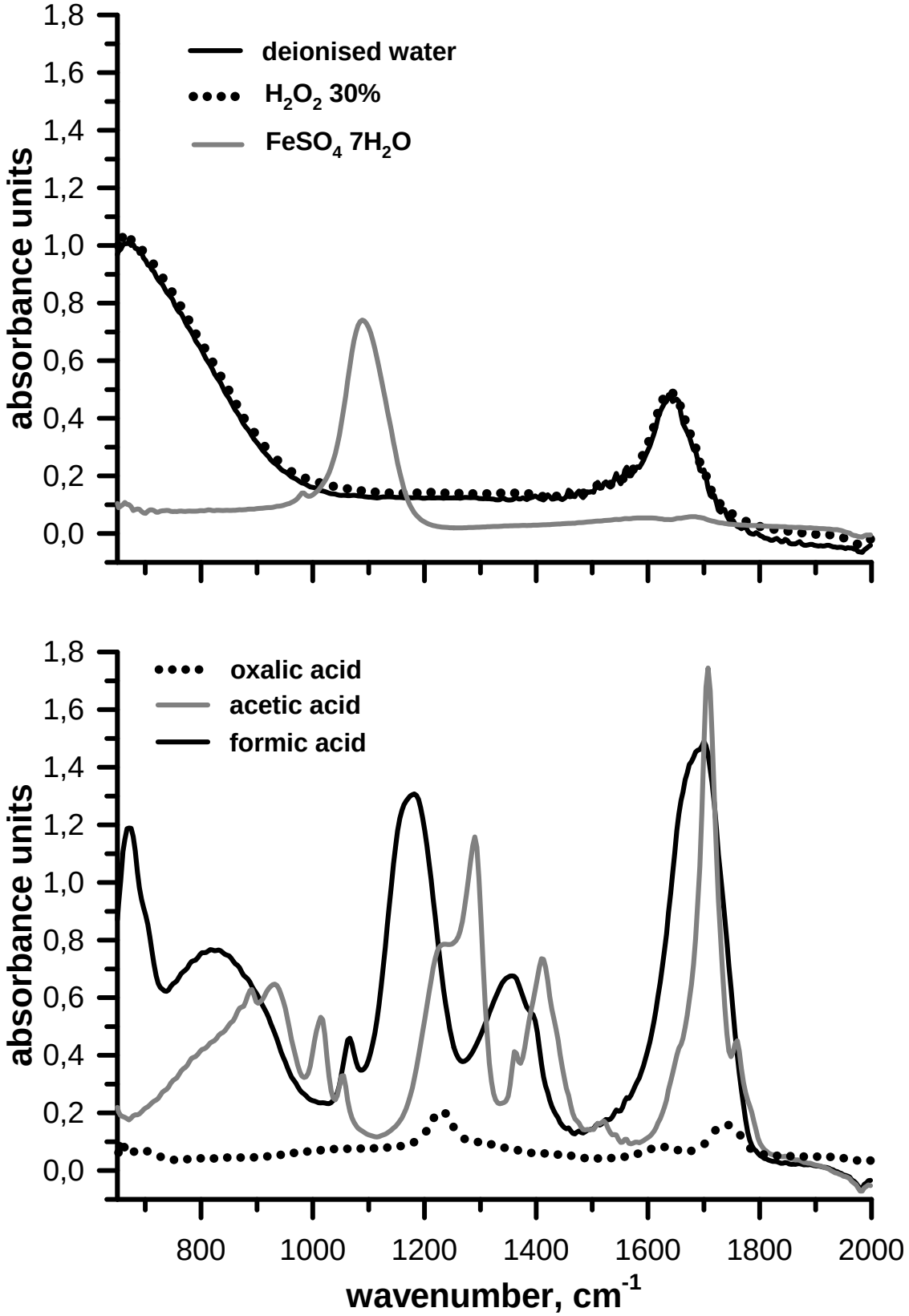
deionised water
H2O2 30%
FeSO4 7H2O
absorbance units
1,8
1,6
1,4
1,2
1,0
0,8
0,6
0,4
0,2
0,0
oxalic acid
acetic acid
formic acid
absorbance units
800
1000
1200
1400
1600
1800
2000
wavenumber, cm-1

FIGURE A.2.

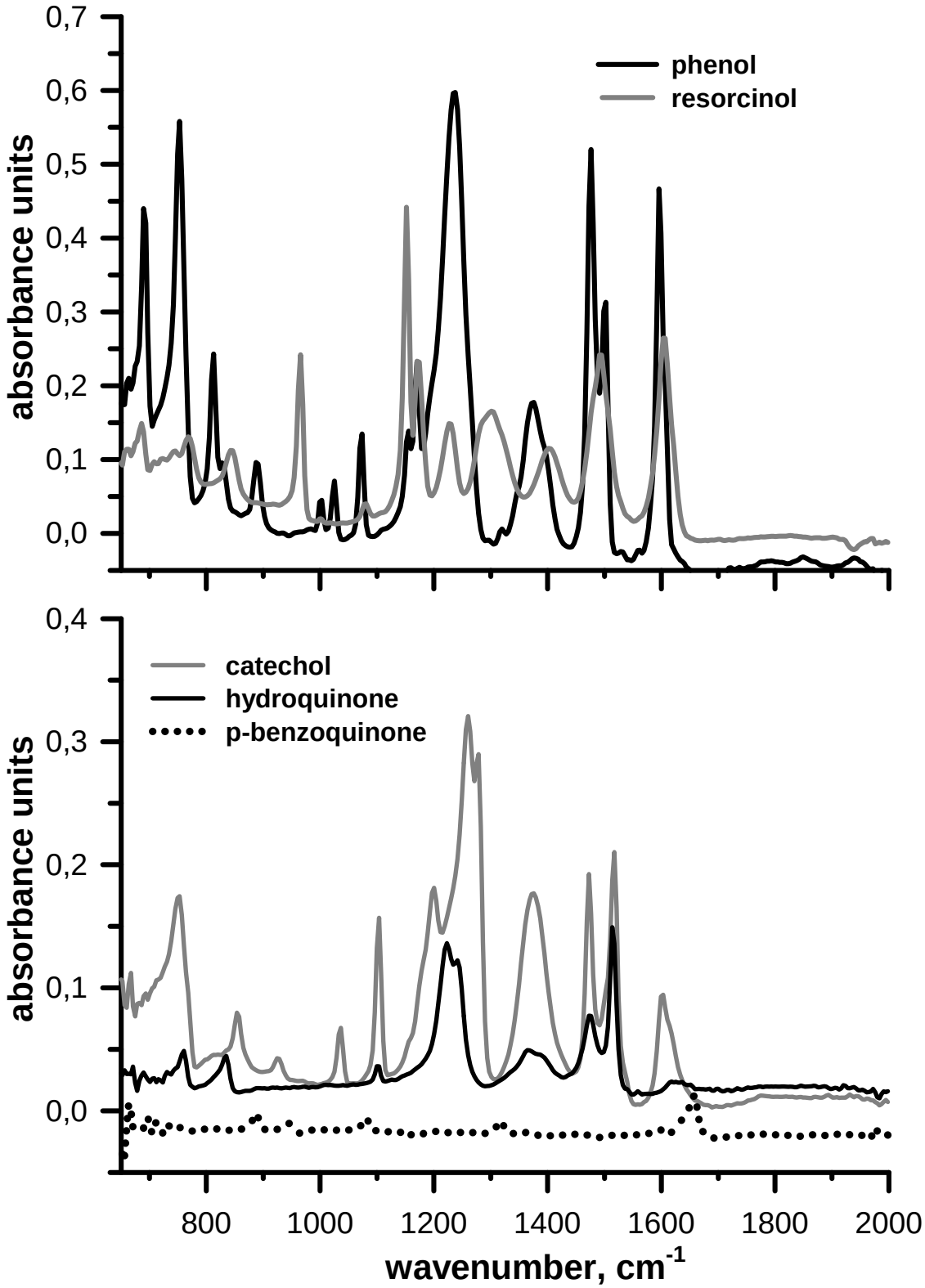
phenol
resorcinol
absorbance units
0,7
0,6
0,5
0,4
0,3
0,2
0,1
0,0
catechol
hydroquinone
p-benzoquinone
absorbance units
0,4
0,3
0,2
0,1
0,0
800
1000
1200
1400
1600
1800
2000
wavenumber, cm-1

FIGURE 1

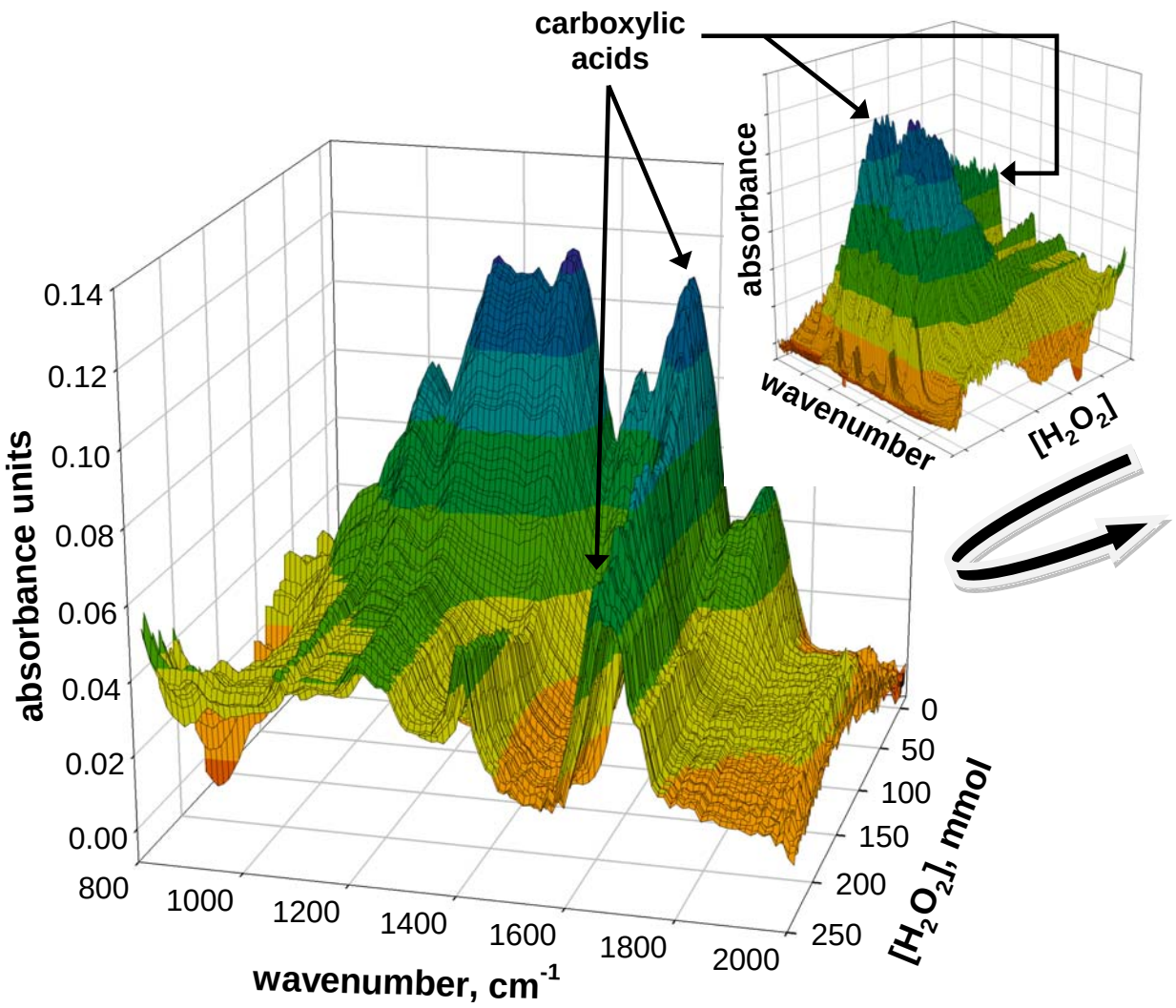
carboxylic acids
absorbance
wavenumber
[H2O2]
absorbance units
0.14
0.12
0.10
0.08
0.06
0.04
0.02
0.00
800
1000
1200
1400
1600
1800
2000
wavenumber, cm-1
0
50
100
150
200
250
[H2O2], mmol

FIGURE 2

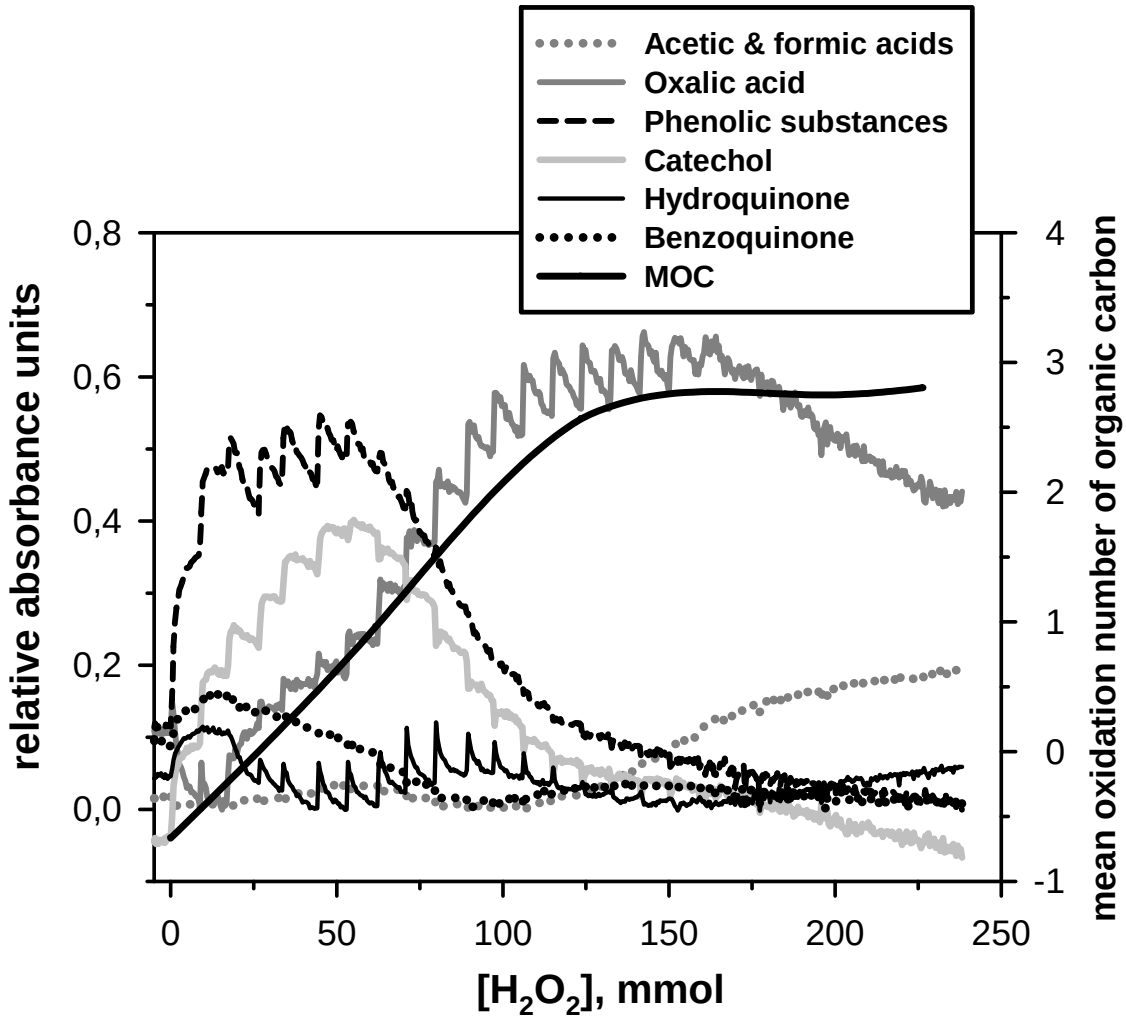
Acetic & formic acids
Oxalic acid
Phenolic substances
Catechol
Hydroquinone
Benzoquinone
MOC
relative absorbance units
mean oxidation number of organic carbon
0,0
0,2
0,4
0,6
0,8
-1
0
1
2
3
4
0
50
100
150
200
250
[H2O2], mmol

FIGURE 3

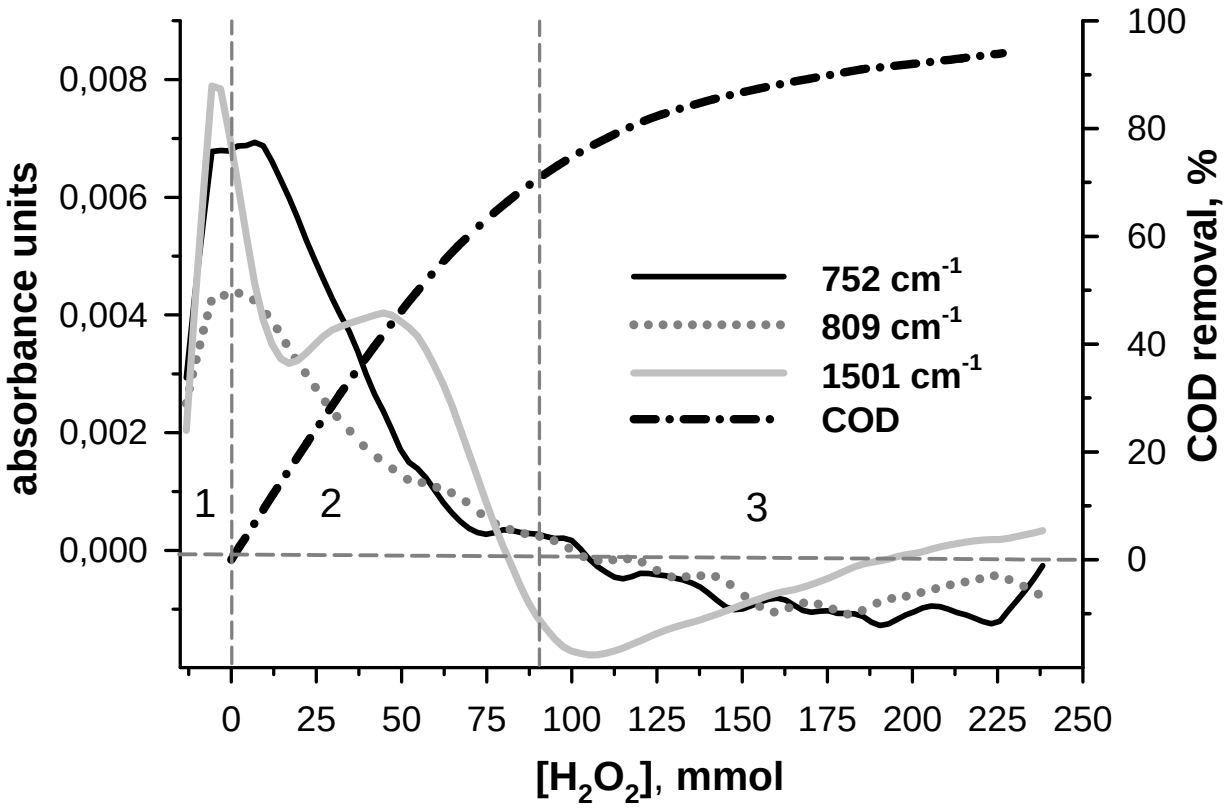
absorbance units
0,008
0,006
0,004
0,002
0,000
COD removal, %
100
80
60
40
20
0
752 cm-1
809 cm-1
1501 cm-1
COD
1
2
3
0
25
50
75
100
125
150
175
200
225
250
[H2O2], mmol

FIGURE 4

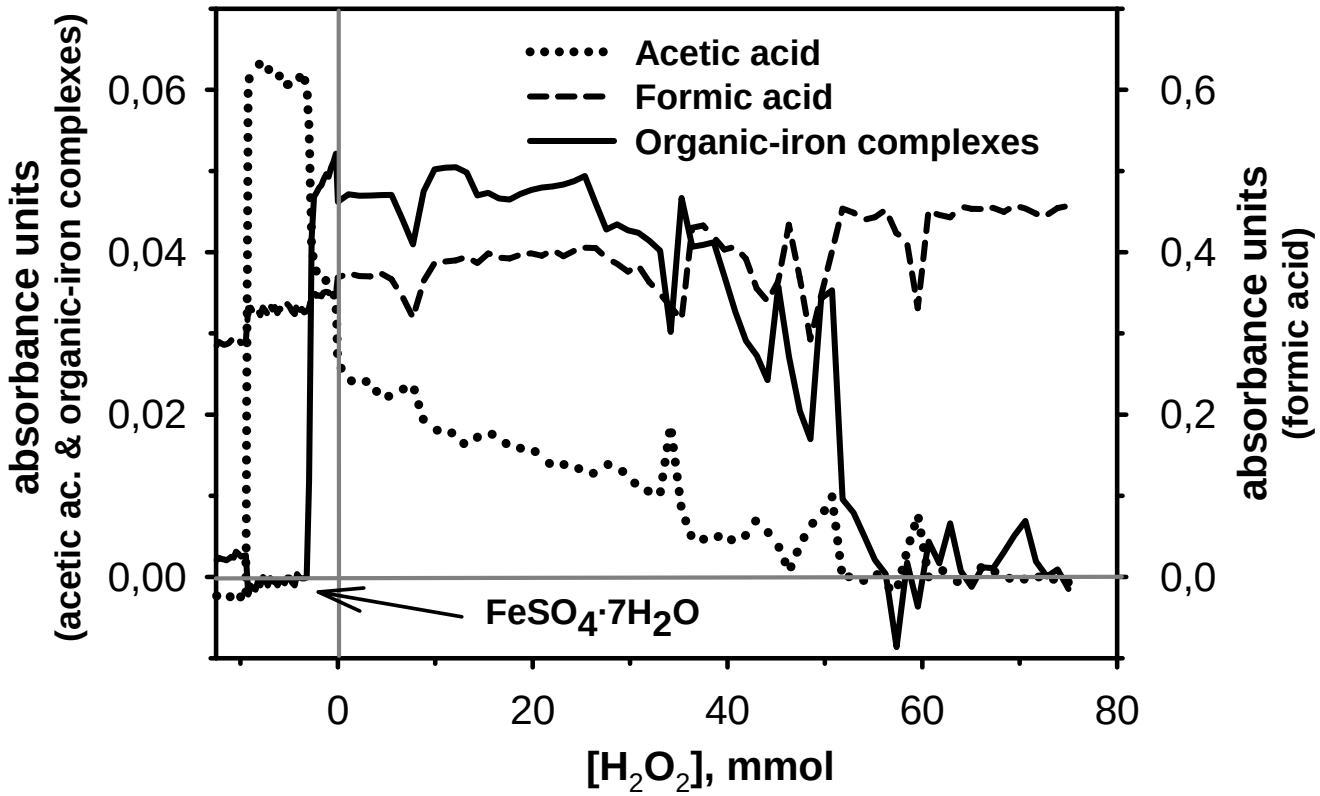
Acetic acid
Formic acid
Organic-iron complexes
absorbance units
(acetic ac. & organic-iron complexes)
absorbance units
(formic acid)
0,06
0,04
0,02
0,00
0,6
0,4
0,2
0,0
FeSO4·7H2O
0
20
40
60
80
[H2O2], mmol

FIGURE 5

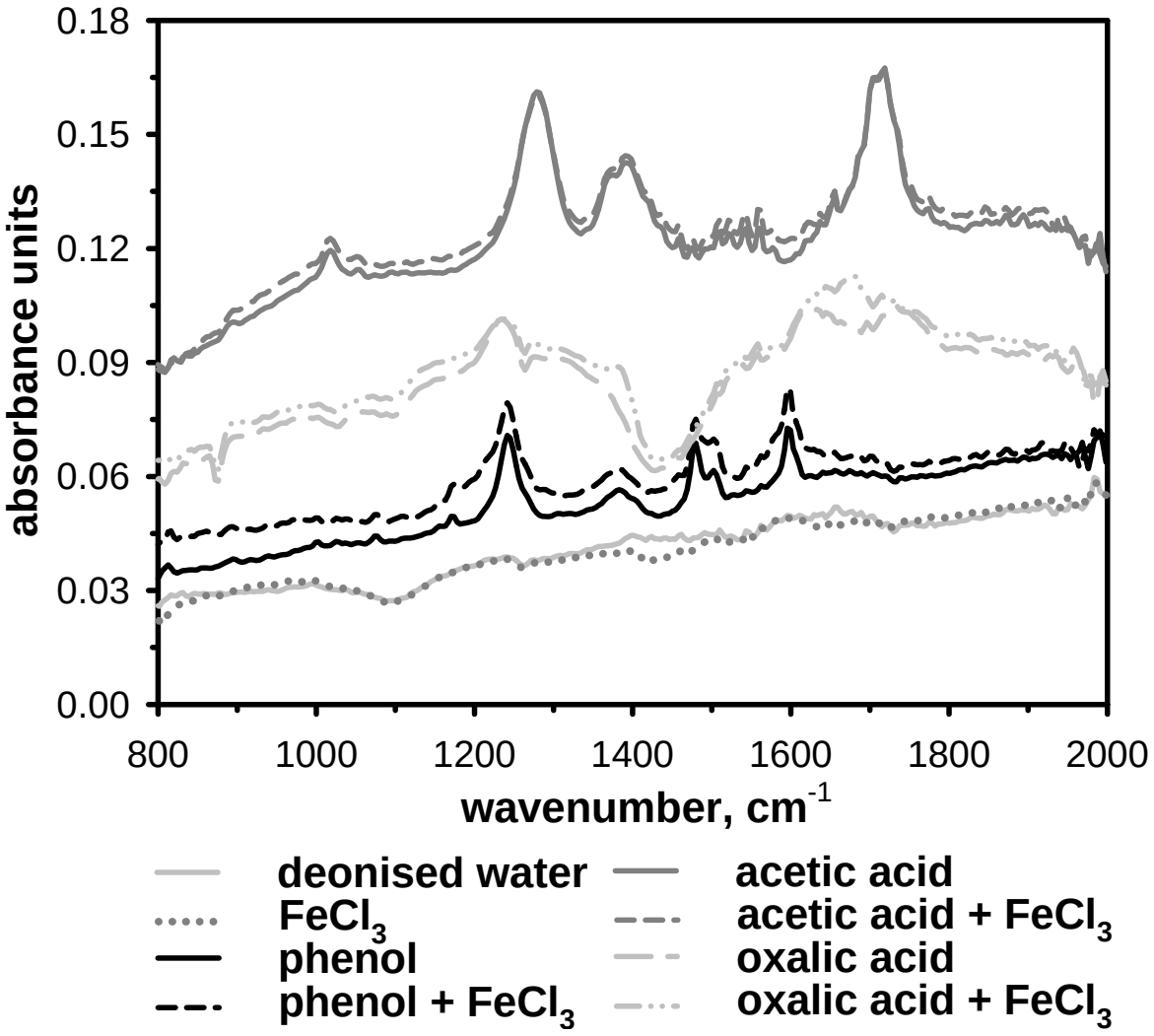
0.18
0.15
0.12
0.09
0.06
0.03
0.00
absorbance units
800
1000
1200
1400
1600
1800
2000
wavenumber, cm-1
deonised water
acetic acid
FeCl3
acetic acid + FeCl3
phenol
oxalic acid
phenol + FeCl3
oxalic acid + FeCl3

FIGURE 6

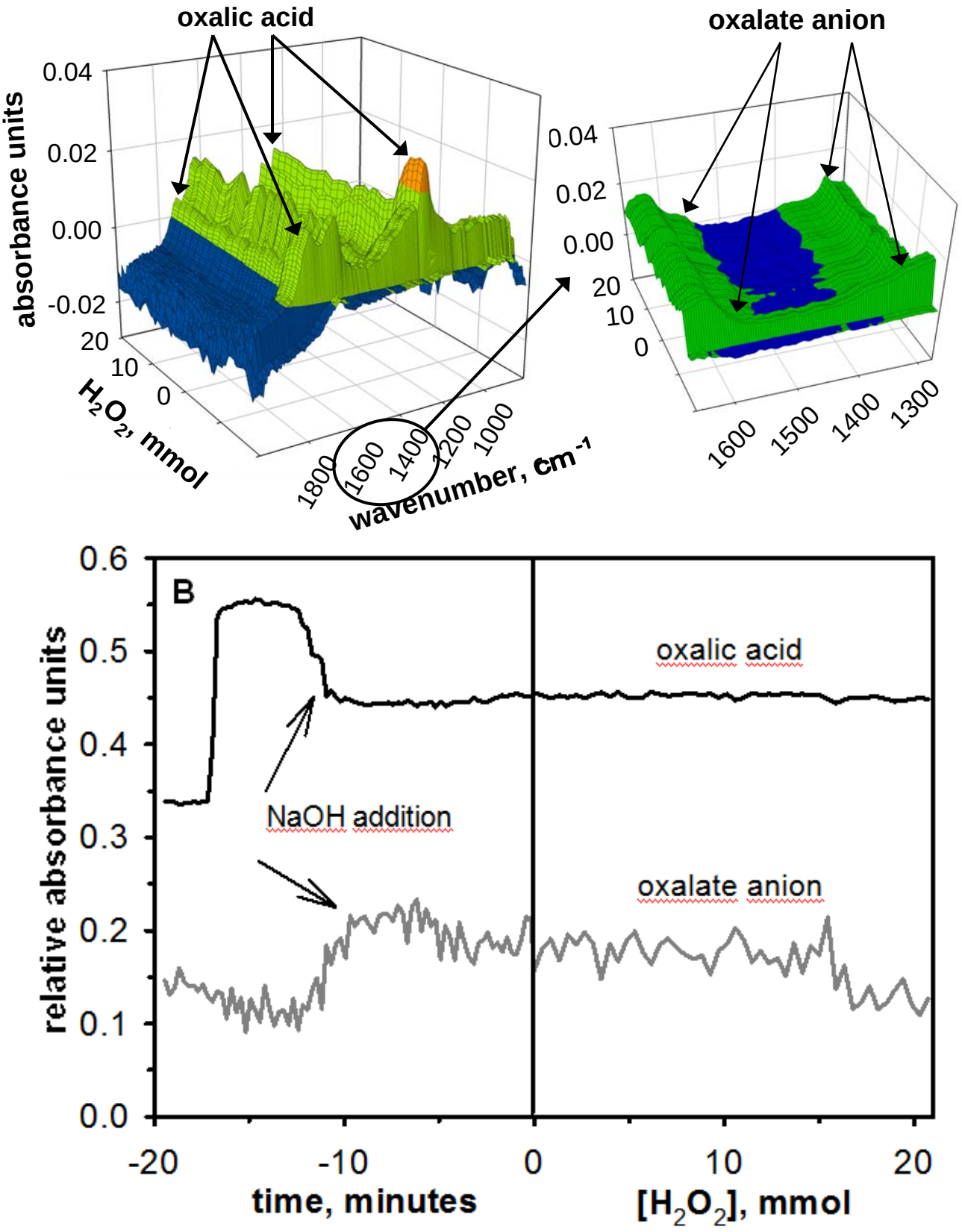
oxalic acid
oxalate anion
absorbance units
0.04
0.02
0.00
-0.02
20
10
0
H_2O_2, mmol
1800
1600
1400
1200
1000
wavenumber, cm^{-1}
1600
1500
1400
1300
B
relative absorbance units
0.6
0.5
0.4
0.3
0.2
0.1
0.0
oxalic acid
NaOH addition
oxalate anion
-20
-10
0
10
20
time, minutes
$[H_2O_2]$, mmol

FIGURE 7

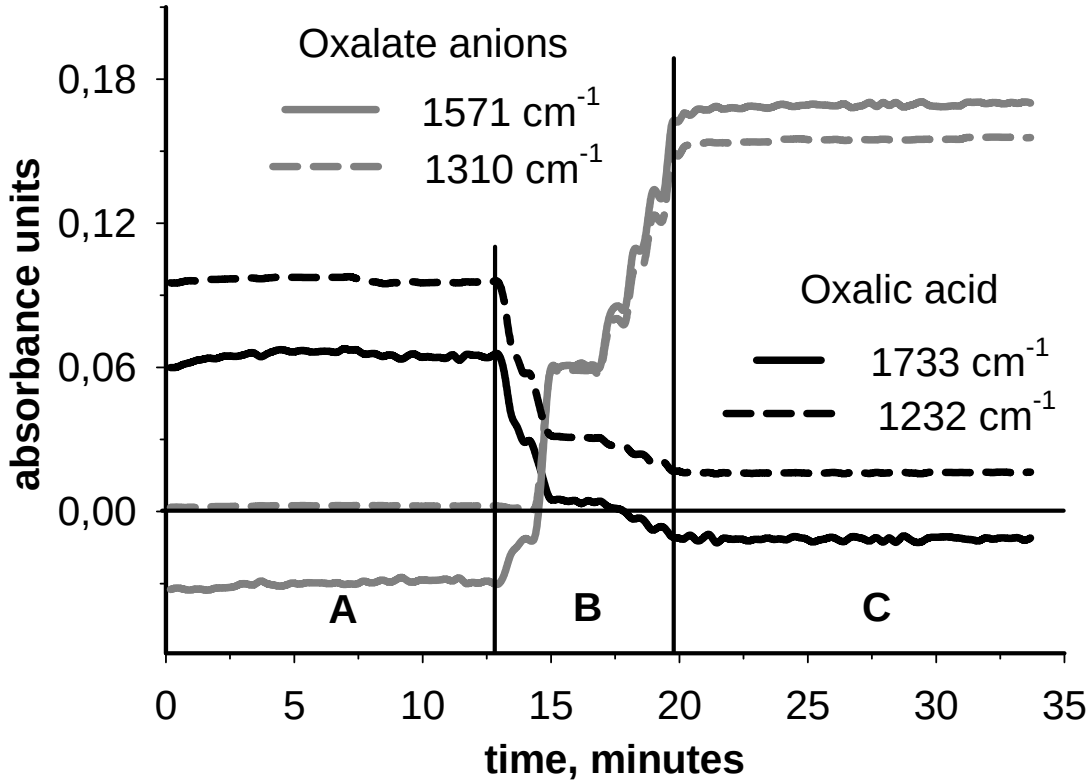
Oxalate anions
1571 cm-1
1310 cm-1
Oxalic acid
1733 cm-1
1232 cm-1
absorbance units
0,18
0,12
0,06
0,00
A
B
C
0
5
10
15
20
25
30
35
time, minutes